Electronic Supplementary Material (ESI) for New Journal of Chemistry.

Supporting Information for

Mediating the Li Diffusion Path in Composite Polymer Electrolytes by mesoporous SBA-15 for All-Solid-State Lithium Batteries

Jinqiu Huang[1#], Lei Xu[1#], Tianshi Feng[1], Yubing Hu[1], Lifeng Zhang[1]* and Langli Luo[1,2]*

[1]Institute of Molecular Plus, Tianjin University, Tianjin, 300072, P. R. China

[2]Haihe Laboratory of Sustainable Chemical Transformations, Tianjin 300192 (China)

[#]Equally contributed first authors.

*Corresponding Authors: **Dr. Lifeng Zhang** (lfzhang007@tju.edu.cn); **Dr. Langli Luo** (luolangli@tju.edu.cn)

Experimental Details

Fabrication of SBA-15 and PEO composite polymer electrolytes

The poly(ethylene oxide) (PEO, Mw = 600000, Aladdin) and lithium bis(trifluoromethanesulfonyl) imide (LiTFSI, ≥98.0 %, D&B) were dried at 70 °C in vacuum for 24 h to remove the absorbed air and water and then transferred to an Ar-filled glovebox(H_2O ≤0.01 ppm and O_2 ≤ 0.01 ppm). SBA-15 (XF Nano, China) was used without further treatment.

First, certain mass of SBA-15 was dissolved in 6mL acetonitrile (CH_3CN, >99 %, Aladdin) and dispersed evenly by ultrasonic for 20min. Thereafter, 0.3g PEO and 0.15g LiTFSI (EO : Li^+ = 13) were added under the condition of stirring, and stirred vigorously for 24 h to make the mixture uniform. Finally, the mixture was cast to a PTFE plate and dried at 60 °C in vacuum for 48 h. The membrane was stored in an Ar-filled glove box until cells were prepared. The proportion of SBA-15 was set to 0 wt%, 2 wt%, 5 wt%, 10 wt% and 15 wt% (weight percentage), respectively. The obtained electrolyte contains X% content of SBA-15 is denoted as X% SBA-15 CPE. The PEO solid polymer electrolyte (PEO SPE) is fabricated with above method without SBA-15.

Electrode Preparation

To fabricate $LiFePO_4$ cathode, the active material $LiFePO_4$, conductive carbon black, and binder poly(vinylidene difluoride) (PVDF) (weight ratio 8:1:1) were dissolved in 1-methyl-2-pyrrolidinone (NMP) and stirred for 4 h. Then the slurry was cast on Al foil and dried at 80 °C in vacuum for 12 h. The active material area mass is about 2 mg

cm^{-2} .

Materials Characterization.

The specific surface area and pore size distribution of SBA-15 were measured by the Brunauer−Emmett−Teller (BET, ASAP2460) and Barrett−Joyner−Halenda (BJH) methods. The crystalline phases of SBA-15, SPE and CPEs were determined by small angle X-ray diffraction (SAXD, MiniFlex600) from 0.5° to 5° and wide angle X-ray diffraction (WAXD, MiniFlex600) from 5° to 60° using Cu Kα radiation. The morphologies of SBA-15, the top-view and the cross-sectional of CPEs were observed by Field emission scanning electron microscopy (FESEM, Apreo S LoVac) and High-resolution transmission electron microscopy (TEM, ThermoFisher® Talos F200X). The elemental mappings of SBA-15 and LiTFSI in the CPEs were distinguished by energy dispersive spectrometry (EDS, Bruker XFlash6|60). The mechanical properties of PEO SPE and 5%SBA-15 CPE were characterized by nano indentation test (Nano Test vantage). The cross-section of the sample is prepared by brittle fracture with liquid nitrogen. The glass transition temperature and crystallization behaviors of PEO, SPE and CPEs were characterized by differential scanning calorimetry (DSC, Q2000 TA Instruments) in the temperature range of -80 to 100 °C, 10 °C min^{-1} as the heating rate. The thermal property of SPE and CPEs was studied by thermogravimetric analysis (TGA , TG 209F3) under Ar atmosphere from 40-800 °C with a heating rate of 10 °C/min. The interaction of components of CPEs was evaluated by Fourier transform infrared spectra (FT-IR, Nicolet IN10). The chemical states of ^{7}Li were tested by solid-state nuclear magnetic resonance (SSNMR, JEOL JNM ECZ600R).

Electrochemical measurements.

The ionic conductivities of electrolytes were measured by electrochemical impedance spectroscopy (EIS, Bio-logic SP-200) at a frequency range from 7 MHz to 0.1 Hz and the temperature range from 20 °C to 70 °C. The electrolyte membranes were sandwiched between the two stainless steel (SS) disks to form a SS/ electrolyte /SS structured cell. The ionic conductivity (σ) was calculated by the following equation:

$$\sigma = \frac{L}{RS} \tag{1}$$

Where L (cm) is the thickness of the electrolyte membrane, R (Ω) is the bulk resistance of the electrolyte membrane and S (cm^2) is the area of the stainless steel. The lithium ion migration number (t_{Li^+}) of the electrolyte was tested by AC impedance and DC polarization for symmetric cell (Li/ electrolyte /Li), and calculated by the following equation:

$$t_{Li+} = \frac{I_s(\Delta V - I_0 R_0)}{I_0(\Delta V - I_s R_s)} \tag{2}$$

Where I_0 and I_s are the initial and steady state current, respectively. R_0 and R_s reflect the interface resistances before and after the polarization. ΔV is the DC potential of 10 mV to be adopted. The electrochemical stability window of electrolytes was tested by linear sweep voltammetry (LSV) using the SS/ electrolyte /Li coin cell at a scan rate of 1 mV s^{-1} from 2.0 to 6.0 V at 60 °C. The interface compatibility between electrolyte and electrode was measured the symmetric battery Li/ electrolyte /Li using EIS with frequency from 7 MHz to 0.1 Hz at 60 °C.

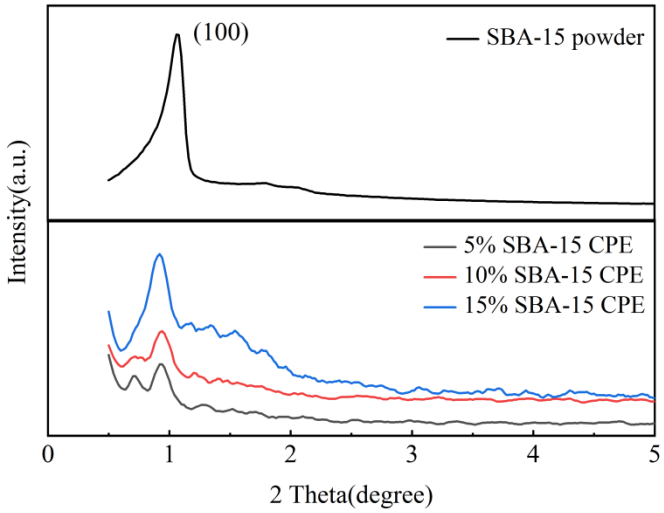

Figure S1. The XRD patterns of (a) SBA-15 power and (b) SBA-15 CPEs with different content of SBA-15.

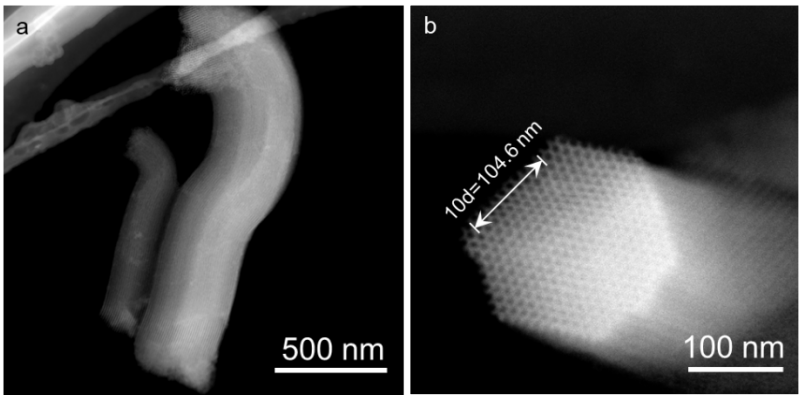

Figure S2. High-resolution HAADF-STEM images showing the highly ordered mesoporous structure of SBA-15. (a) Surface-macroscopic and (b) cross-sectional morphology of one SBA-15.

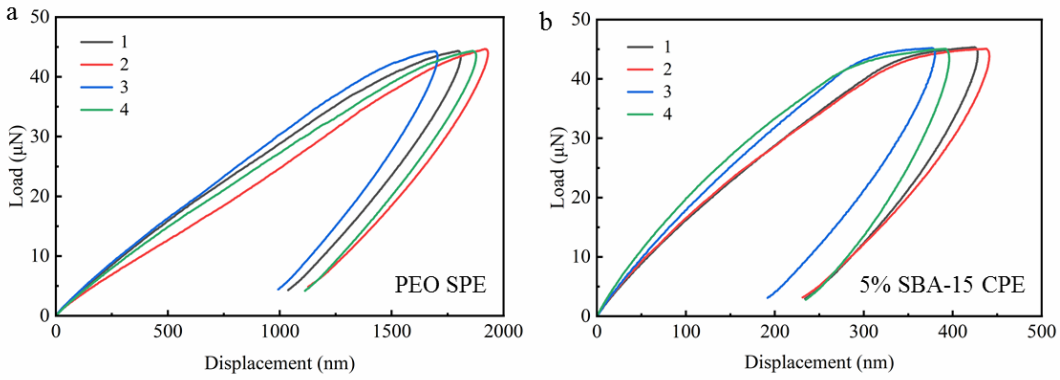

Figure S3. The load-displacement curves of (a) PEO SPE and (b) 5% SBA-15 CPE (Four points were taken from each membrane).

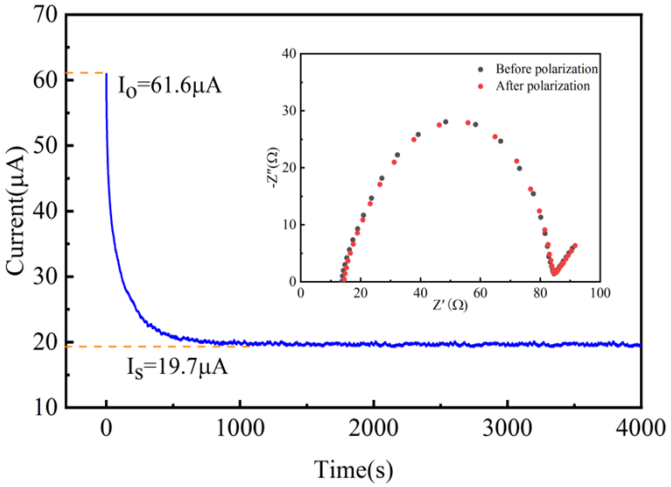

Figure S4. The lithium ion migration number of PEO SPE at 60 °C.

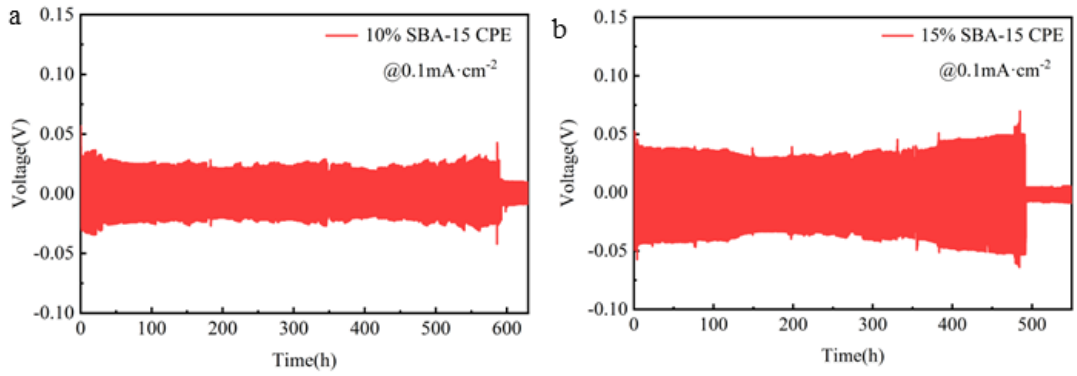

Figure S5. Voltage−time profile of Li metal plating and stripping in (a) Li/10% SBA-15 CPE/Li cell and (b) Li/15% SBA-15 CPE/Li cell at 0.1 mA cm^{-2} and 60 °C.

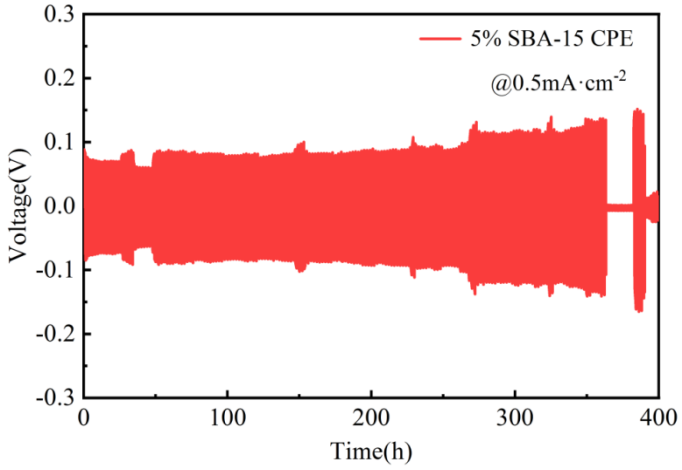

Figure S6. Voltage−time profile of Li metal plating and stripping in Li/5% SBA-15 CPE/Li cell at 0.5 mA cm^{-2} and 60 °C.

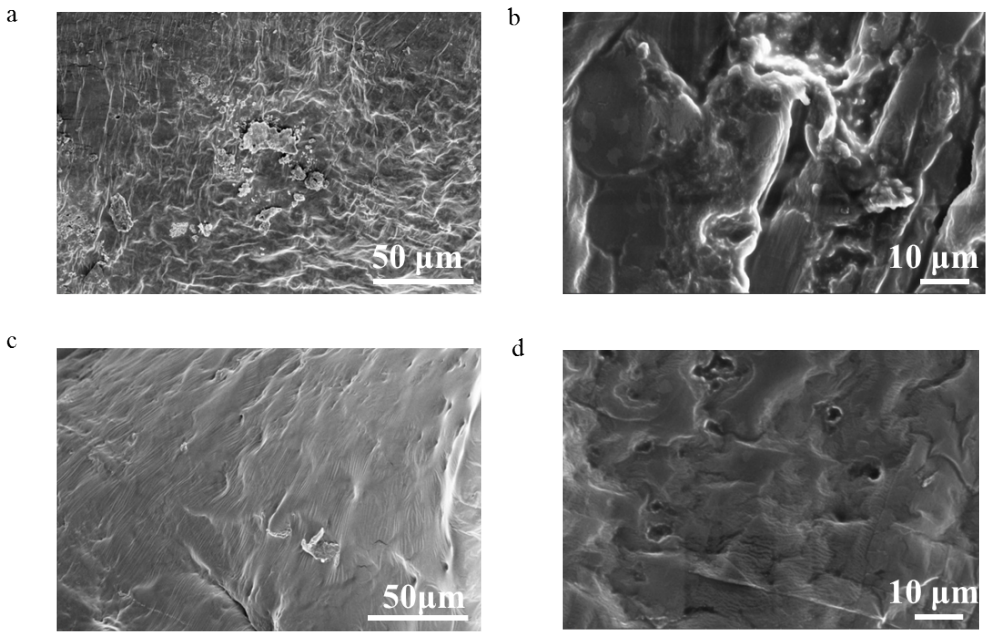

Figure S7. (a) Cross-sectional and surface (b) SEM images of lithium metal in Li/PEO SPE/Li cells after 300 h. (c) Cross-sectional and surface (d) SEM images of lithium metal in Li/5% SBA-15 CPE/Li cells after 800 h.

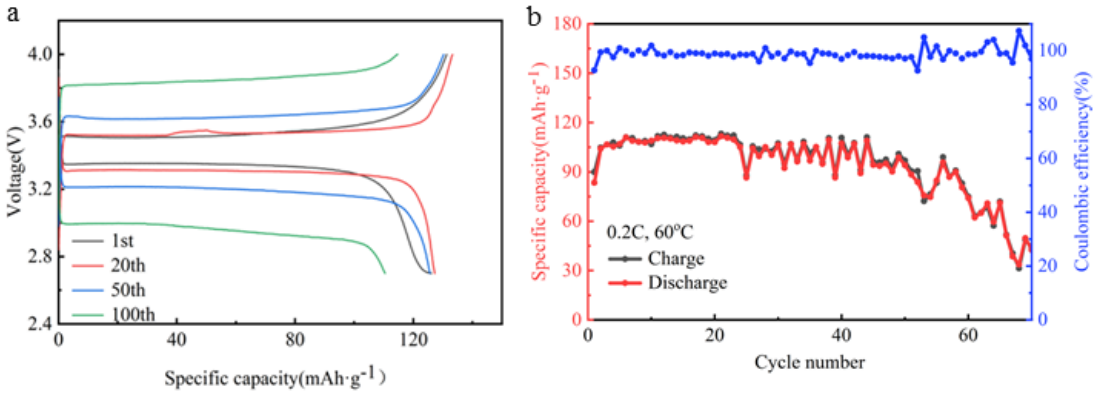

Figure S8. (a) Charge/discharge curves of Li/5% SBA-15 CPE/$LiFePO_4$ at 1st, 20th, 50th and 100th cycles at 0.2 C (60 °C). (b) Cycle performance of Li/PEO SPE/$LiFePO_4$ cells at 0.2 C (60 °C).

Electrolytes	PEO SPE				5% SBA-15 CPE			
Force (μN)	44.5				45			
Depth	1295.87	1356.67	1430.64	1475.80	284.50	322.95	335.26	340.13
Young' modulus (MPa)	8.99	7.83	7.52	7.22	171.86	191.93	148.88	133.02
Hardness (MPa)	0.84	0.77	0.70	0.66	16.81	12.97	12.12	11.70

Table S1. The force, penetration depth, Young's modulus and hardness of PEO SPE and 5% SBA-15 CPE for nano indentation tests at different points.

	peak position (cm^{-1})				
vibrational mode	SBA-15	LiTFSI	PEO	PEO SPE	5% SBA-15 CPE
ν Si-OH	3390				3510
δ O-H	1635				1646
ν_{as} Si−O−Si	1050				1045
ν_{s} Si−O−Si	802				790
ν_{as} SO_2		1338		1345	1342
ν_{s} CF_3		1195			
ν_{s} SO_2		1134			1133
ν_{as} S−N−S		1058			1050
ν_{s} C-H and ν_{as} C-H			2900	2900	2900
δ_{as} CH_2			1465	1465	1465
r_{as} CH_2 and ν C-O-C			964	941	956
r CH_2			845	845	845

[a]Abbreviations of vibration mode: ν = stretching vibration; ν_{as} = asymmetrical stretching vibration; ν_{s} = symmetrical stretching vibration; δ = bending vibration; δ_{as} = asymmetrical bending vibration; r = rooking vibration; r_{as} = asymmetrical rooking vibration

Table S2. Infrared Vibration Mode and Peak Positions of SBA-15, LiTFSI, PEO, PEO SPE and 5% SBA-15 CPE.

Electrolyte compositions	Ionic conductivity	Cathode/anode	Cycle number	Working temp (°C)	Current density	Reference
PEO+PBI	1.8×10^{-4} S cm^{-1}@30 °C	$LiFePO_4$ /Li	100	60	0.2C	1
PEO+UiO-66-NH_2/PAN	4.9×10^{-4} S cm^{-1}@25 °C	$LiFePO_4$ /Li	110	25	0.2C	2
PEO+SN+FEC	3.1×10^{-4} S cm^{-1}@30 °C	NCM532 /Li	120	30	0.1C	3
PEO+LLZO+PTFE	2.54×10^{-4} S cm^{-1}@60 °C	S/Li	100	60	0.1C	4
PEO+ZIF-67	4.33×10^{-4} S cm^{-1}@55 °C	$LiFePO_4$ /Li	100	55	0.5C	5
PEO+LSZP	5.74×10^{-4} S cm^{-1}@25 °C	$LiFePO_4$ /Li	100	25	0.2C	6
PEO+LATP+PI	1.24×10^{-4} S cm^{-1}@30 °C	NCM811/Li	100	30	0.2C	7
PEO+$LiPO_2F_2$	1.9×10^{-4} S cm^{-1}@60 °C	$LiCoO_2$/Li	100	60	0.2C	8
PEO+LALZNO	2.36×10^{-4} S cm^{-1}@60 °C	$LiFePO_4$ /Li	100	60	0.2C	9
PEO+SBA-15	4.26×10^{-4} S cm^{-1}@60 °C	$LiFePO_4$ /Li	110	60	0.2C	this work

Table S3. Comparison of the electrochemical performance of PEO-based electrolytes.

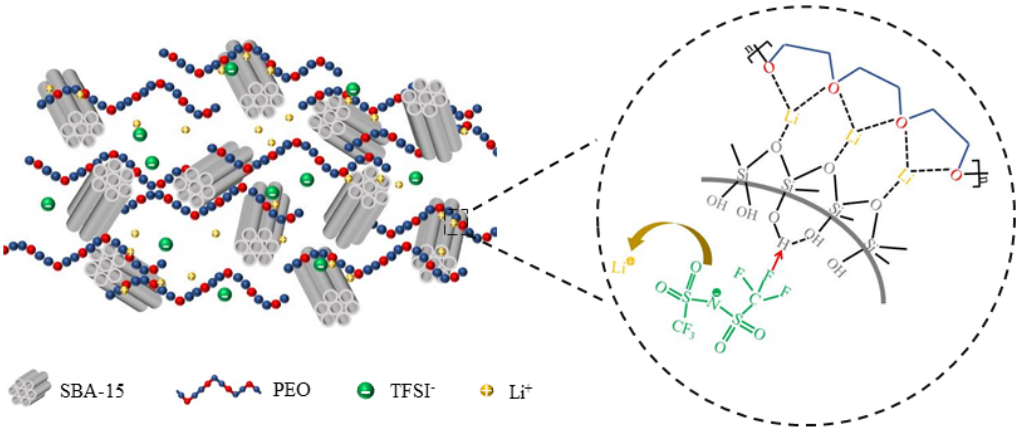

Scheme 1. schematic illustration of the composite polymer electrolyte containing SBA-15. The enlarged part is a proposed mechanism of SBA-15 interaction with PEO and LiTFSI.

References

1. Q. H. Zhang, H. Huang, T. M. Liu, Y. Wang, J. R. Yu and Z. M. Hu, Polymer, 2022, 239.
2. Q. H. Zhang, H. Huang, T. M. Liu, Y. Wang, J. R. Yu and Z. M. Hu, Polymer, 2022, 239.
3. Y. L. Liu, Y. Zhao, W. Lu, L. Q. Sun, L. Lin, M. Zheng, X. L. Sun and H. M. Xie, Nano Energy, 2021, 88.
4. Z. C. Li, T. Y. Li, Y. R. Deng, W. H. Tang, X. D. Wang, J. L. Yang, Q. Liu, L. Zhang, Q. Wang and R. P. Liu, Rare Metals, 2022, 41, 2834-2843.
5. E. Q. Zhao, Y. D. Guo, Y. R. Liu, S. Q. Liu and G. R. Xu, Appl Surf Sci, 2022, 573.
6. H. Park, E. G. Lee, S. Y. Kim, S. J. Seong, J. Y. Suh, M. Y. Wu, Y. K. Kang, S. Y. Choi, Y. Kim and S. Choi, Acs Appl Energ Mater, 2021, 4, 13974-13982.
7. H. Park, E. G. Lee, S. Y. Kim, S. J. Seong, J. Y. Suh, M. Y. Wu, Y. K. Kang, S. Y. Choi, Y. Kim and S. Choi, Acs Appl Energ Mater, 2021, 4, 13974-13982.
8. J. X. Tan, X. H. Li, Q. H. Li, Z. X. Wang, H. J. Guo, G. C. Yan, J. X. Wang and G. C. Li, Ionics, 2022, 28, 3233-3241.
9. R. M. Wang, F. Liu, J. F. Duan, Y. Ren, M. J. Li and J. X. Cao, Acs Appl Energ Mater, 2021, 4, 13912-13921.